Observation of Many-Body Localization in a One-Dimensional System with a Single-Particle Mobility Edge

Thomas Kohlert,[1,2,3,*] Sebastian Scherg,[1,2,3,*] Xiao Li,[4,5,*] Henrik P. Lüschen,[1,2] Sankar Das Sarma,[4] Immanuel Bloch,[1,2,3] and Monika Aidelsburger[1,2,3,†]

[1]*Fakultät für Physik, Ludwig-Maximilians-Universität München, Schellingstraße 4, 80799 München, Germany*
[2]*Max-Planck-Institut für Quantenoptik, Hans-Kopfermann-Straße 1, 85748 Garching, Germany*
[3]*Munich Center for Quantum Science and Technology (MCQST), Schellingstraße 4, 80799 München, Germany*
[4]*Condensed Matter Theory Center and Joint Quantum Institute, University of Maryland, College Park, Maryland 20742-4111, USA*
[5]*Department of Physics, City University of Hong Kong, Kowloon, Hong Kong, China*

(Received 28 September 2018; published 3 May 2019)

We experimentally study many-body localization (MBL) with ultracold atoms in a weak one-dimensional quasiperiodic potential, which in the noninteracting limit exhibits an intermediate phase that is characterized by a mobility edge. We measure the time evolution of an initial charge density wave after a quench and analyze the corresponding relaxation exponents. We find clear signatures of MBL when the corresponding noninteracting model is deep in the localized phase. We also critically compare and contrast our results with those from a tight-binding Aubry-André model, which does not exhibit a single-particle intermediate phase, in order to identify signatures of a potential many-body intermediate phase.

DOI: 10.1103/PhysRevLett.122.170403

Introduction.—In the past decade, it has been established that an isolated one-dimensional (1D) quantum system with strong quenched disorder can be localized, even if finite interactions are present [1–19]. Such a phenomenon, now known as many-body localization (MBL), represents a generic example of ergodicity breaking in isolated quantum systems. In particular, the eigenstate thermalization hypothesis (ETH) [20,21] is strongly violated in such systems, leading to the inapplicability of textbook quantum statistical mechanics. Recently, experiments have found strong evidence for the existence of an MBL phase in interacting 1D systems with random disorder [22–24] and in models with quasiperiodic potentials [25,26] captured by the Aubry-André (AA) tight-binding lattice model [7,27,28]. One hallmark of the noninteracting AA model is that the localization transition occurs sharply at a single disorder strength. As a result, across the transition, all single-particle eigenstates in the spectrum suddenly become exponentially localized without mobility edges.

In contrast, there are many other 1D models which exhibit a single-particle mobility edge [29–37], i.e., a critical energy separating extended and localized eigenstates in the spectrum. As a result, a single-particle intermediate phase (SPIP) characterized by a coexistence of localized and extended eigenstates in the energy spectrum appears in the phase diagram (Fig. 1). Experimental signatures of such an intermediate phase have been recently observed using ultracold atomic gases in a 1D quasiperiodic optical lattice described by a generalized Aubry-André (GAA) model including next-nearest-neighbor tunneling [38,39], as well as in a momentum-space lattice [40]. In the presence of interactions, two natural questions arise. (i) Does an MBL phase exist in a model, which in the limit of vanishing interactions exhibits an SPIP? This question has been addressed in several numerical studies, predicting MBL in some cases but not in others [13,41]. Definite conclusions, however, are often challenged by finite-size effects. (ii) Does the SPIP survive finite interactions to become a many-body intermediate phase (MBIP)? This would suggest the existence of an intermediate phase, where extended and localized many-body

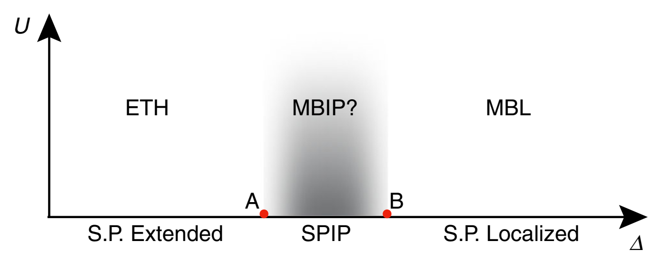

FIG. 1. Heuristic phase diagram of the GAA model: The noninteracting GAA model exhibits three phases (single-particle extended, SPIP, and single-particle localized), with the phase boundary denoted by A and B. Here Δ is the strength of the detuning lattice [Eq. (2)], while U is the strength of the Hubbard on-site interactions [Eq. (4)]. The situation with finite interactions is unknown in theory, although a full MBL phase is believed to exist in the regime, where the corresponding noninteracting system is single-particle localized. Below the single-particle localization transition point A, interactions will lead to a thermal phase, where the ETH holds. The existence of an MBIP (marked in gray) is highly debated.

 © 2019 American Physical Society

states coexist in the energy spectrum [15,16,42,43]. Note that this does not necessarily require the existence of a many-body mobility edge; instead, a coexistence of localized and extended many-body states at a fixed energy density has been predicted in certain models [43]. The existence of an MBIP is highly debated in theory [44,45], although there have been extensive numerical simulations in the literature asserting the existence of an MBIP in various different systems [9–17,42,43,46–49]. Given the direct observation of the SPIP in recent experiments [39,40], this issue takes on immediate experimental significance regarding the fate of this noninteracting intermediate phase as interactions are added.

In this work, we address the two questions raised above by studying quench dynamics from an initial charge-density wave (CDW) [25] with ultracold fermionic atoms in a quasiperiodic optical lattice in a large system with more than 100 lattice sites. We investigate the relaxation dynamics in the interacting GAA model and contrast them with the interacting AA model, which has been studied in previous works [25,50]. The GAA model takes the continuum limit of the AA tight-binding lattice model and contains next-nearest-neighbor tunnel couplings. This breaks the self-duality of the AA model and, therefore, leads to the appearance of an intermediate phase in the noninteracting regime [39]. In the presence of interactions, the nature of the phase diagram of the GAA model is unknown (Fig. 1). Although MBL is believed to exist in this system, it has not been verified in experiments. We obtain two main results: (i) We establish the existence of MBL in a new model, i.e., the GAA model, in a regime where its noninteracting counterpart is fully localized; (ii) we find no discernible difference in the relaxation dynamics between the interacting GAA and AA model for all system parameters within the experimentally accessible timescales.

Experiment.—Our experimental system consists of a primary lattice with a wavelength of $\lambda_p = 532$ nm and two deep orthogonal lattices at a wavelength of 738 nm, which divide the atomic cloud into an array of 1D tubes with lattice spacing $d = \lambda_p/2$. The full-width-half-maximum size of the cloud is about 150 lattice sites with an average filling of ~0.5 atoms per lattice site. A detuning lattice ($\lambda_d = 738$ nm) incommensurate with the primary lattice introduces quasiperiodicity and enables the realization of both the AA and the GAA models, depending on the primary lattice depth. In the noninteracting limit, such a system is described by the following continuum Hamiltonian (incommensurate lattice model):

$$\hat{H} = -\frac{\hbar^2}{2m}\frac{d^2}{dx^2} + \frac{V_p}{2}\cos(2k_p x) + \frac{V_d}{2}\cos(2k_d x + \phi), \quad (1)$$

where $k_i = 2\pi/\lambda_i$ ($i = p,\ d$) is the wave vector of the corresponding lattice, m is the mass of the atoms, V_i ($i = p,\ d$) is the respective lattice depth, and ϕ is the relative phase between the primary and detuning lattice. We will use the recoil energy of the primary lattice $E_r^p = \hbar^2 k_p^2/(2m)$ with the reduced Planck constant $\hbar$ as the energy unit throughout this work.

In the tight-binding limit (i.e., when the primary lattice potential V_p is deep), the continuum Hamiltonian in Eq. (1) maps onto the tight-binding 1D AA model:

$$\hat{H}_{\mathrm{AA}} = -J_0 \sum_{j,\sigma} (\hat{c}^\dagger_{j+1,\sigma}\hat{c}_{j,\sigma} + \mathrm{H.c.}) + \Delta \sum_{j,\sigma} \cos(2\pi\alpha j + \phi)\hat{n}_{j,\sigma}, \quad (2)$$

which describes our experiment sufficiently well at a primary lattice depth $V_p \gtrsim 8E_r^p$ [39]. In the above Hamiltonian, J_0 is the nearest-neighbor hopping energy, and Δ is the strength of the detuning lattice. The operator $\hat{c}^\dagger_{j,\sigma}$ ($\hat{c}_{j,\sigma}$) denotes the creation (annihilation) operator for spin $\sigma = \uparrow, \downarrow$ on lattice site j, and $\hat{n}_{j,\sigma} = \hat{c}^\dagger_{j,\sigma}\hat{c}_{j,\sigma}$ is the corresponding fermion number operator. The incommensurability $\alpha = \lambda_p/\lambda_d \simeq 532/738$ is the ratio of primary and detuning lattice wavelengths. The noninteracting AA model [Eq. (2)] is well known to have a localization transition at $\Delta = 2J_0$, when all energy eigenstates convert from being extended to localized [7].

Beyond the tight-binding limit, corrections have to be added to the AA model. These corrections can be derived via a Wegner flow approach [38], leading to a GAA model Hamiltonian $\hat{H}_{\mathrm{GAA}} = \hat{H}_{\mathrm{AA}} + \hat{H}'$, with

$$\hat{H}' = J_1 \sum_{j,\sigma} \cos\left[2\pi\alpha\left(j + \frac{1}{2}\right) + \phi\right](\hat{c}^\dagger_{j+1,\sigma}\hat{c}_{j,\sigma} + \mathrm{H.c.}) - J_2 \sum_{j,\sigma}(\hat{c}^\dagger_{j+2,\sigma}\hat{c}_{j,\sigma} + \mathrm{H.c.}) + \Delta' \sum_{j,\sigma} \cos(4\pi\alpha j + 2\phi)\hat{n}_{j,\sigma}. \quad (3)$$

For a detailed description of the parameters, see Ref. [51]. Note that the GAA model of Eq. (3) is by definition non-nearest-neighbor and, therefore, cannot be characterized by a single dimensionless parameter Δ/J_0 as in the AA model.

Experimentally, the GAA model is realized with a shallower primary lattice with $V_p = 4E_r^p$ [38,39]. We employ an atom cloud of about 5×10^4 fermionic ^{40}K atoms at a temperature of $0.15(2)T_F$, where T_F is the Fermi temperature in the dipole trap, and load it into the 3D optical lattice. The gas consists of an equal spin mixture of the states $|\uparrow\rangle \equiv |m_F = -7/2\rangle$ and $|\downarrow\rangle \equiv |m_F = -9/2\rangle$ of the $F = 9/2$ ground state hyperfine manifold. On-site interactions can be controlled via a magnetic Feshbach resonance at 202.1 G, resulting in tunable Fermi-Hubbard-type interactions, described by

$$\hat{H}_U = U\sum_j \hat{n}_{j,\uparrow}\hat{n}_{j,\downarrow}. \quad (4)$$

Using a superlattice with wavelength $2\lambda_p$, an initial CDW is created in the primary lattice, where only even sites are occupied and the spin states are randomly distributed [25]. The formation of doubly occupied sites is suppressed by strong repulsive interactions during lattice loading such that the fraction of doublons is below our detection limit [25]. Time evolution is initiated by quenching the primary lattice to a variable depth V_p and simultaneously superimposing the detuning lattice with a strength V_d and phase ϕ relative to the primary lattice. To detect the localization properties of the system, we measure the density imbalance between atoms on even (N_e) and odd (N_o) sites $\mathcal{I} = (N_e - N_o)/(N_e + N_o)$. This quantity is extracted using a band-mapping technique [53,54]. Because of the CDW initial state, a finite steady-state imbalance $\mathcal{I}$ directly signals the presence of localized states through the retention of the initial state memory following the quench.

Time evolution of the imbalance.—Many theoretical studies have focused on the regime of weak interactions $U/J_0 \leq 1$ searching for an MBL phase as well as an MBIP [10,13,15,16,35,38,46,49]. In this work, we measure the imbalance as a function of time for a fixed interaction strength $U/J_0 = 1$ and various detuning lattice strengths V_d in the AA and GAA model. The imbalance is monitored between 10τ and 100τ for the GAA model or between 10τ and 40τ for the AA model, where $\tau = \hbar/J_0$ is the tunneling time in the respective model. The different measurement times are due to the different values of τ in the two models, since they differ in the primary lattice depth (see Ref. [51]). Note that the actual measurement time of about 10 ms is approximately identical for both models, as it is limited by the presence of residual external baths acting independently of the studied model [55,56]. We omit the initial dynamics of the imbalance at $t < 10\tau$ showing damped oscillations accompanied by a rapid decay from the starting value $\mathcal{I}(t = 0) = 0.90(2)$ [25,50].

In Fig. 2, we present a comparison of the time traces for both models for two different detuning lattice strengths on a doubly logarithmic scale. The single-particle localization transition of the AA model and the extended-to-SPIP transition in the GAA model are both located at roughly $\Delta/J_0 = 2$ [27,38,51]. Below the transition, the imbalance decays to zero quickly within a few tunneling times due to the absence of localized states. Therefore, we focus on detuning lattice strengths larger than the critical detuning $\Delta/J_0 = 2$. In the weakly interacting regime ($U/J_0 = 1$), we find that the time traces at a weak detuning strength ($\Delta/J_0 = 2.1$), just above the single-particle localization transition [51], exhibit a considerable imbalance decay over the observation time, irrespective of the underlying model. The second set of traces ($\Delta/J_0 = 3.1$) in Fig. 2 is recorded deep in the localized phase of both corresponding noninteracting models. We find that the imbalance decay in the second set is much slower compared to the first one, and the overall imbalance values are distinctly larger at all measurement times in the second set. This is again valid for the AA as well as the GAA model. The experimental data are in reasonable agreement with exact diagonalization simulations with eight spinful particles on 16 lattice sites, which were averaged for random initial spin configurations [51]. The offset is most likely caused by the harmonic trap present in the experiment [25].

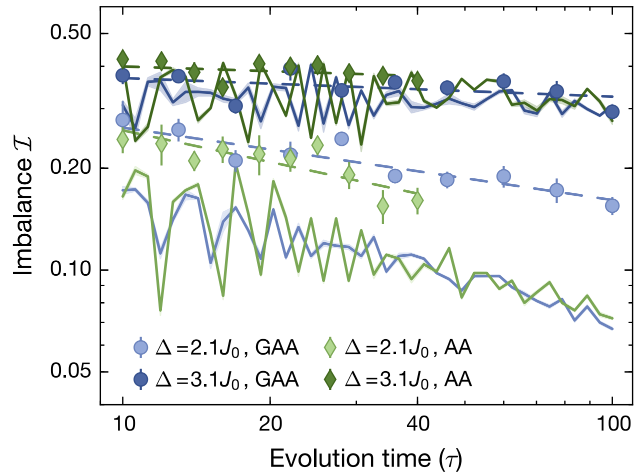

FIG. 2. Time evolution of the imbalance: Measured imbalance time traces in the AA model [$V_p = 8.0(1)E_r^p$] and the GAA model [$V_p = 4.0(1)E_r^p$] at a fixed interaction strength $U/J_0 = 1$. Every data point is averaged over six different detuning phases ϕ, and error bars denote the standard error of the mean. The dashed lines are power-law fits to the experimental data. The solid lines are numerical simulations of the time traces in a system of $L = 16$ sites [51] and the shaded regions indicate numerical uncertainties.

We attribute the different behaviors of the imbalance dynamics of the AA model at different disorders to a many-body localized and many-body extended (i.e., ETH) phase [7,25], above and below an interaction-dependent critical disorder strength, respectively. Because of the remarkably similar dynamics in the GAA model, we infer that MBL exists in this model despite the presence of an SPIP in the noninteracting limit. The data further show that we have a many-body extended phase at weak detuning, while for strong detuning the interacting system is likely many-body localized. Finally, we observe that the imbalance time traces of the two models are indistinguishable within our resolution, both above and below the MBL transition.

Relaxation exponents.—To better quantify the relaxation dynamics, we fit the imbalance time traces using a power-law function $\mathcal{I} \propto t^{-\xi}$ (Fig. 2) and extract the resulting exponents ξ as shown in Fig. 3. Note that a power-law description for a system with quasiperiodic potentials is not motivated by the standard Griffiths description, which is presumably applicable only for randomly disordered systems [18,57–59]. Nonetheless, we find our data to be well

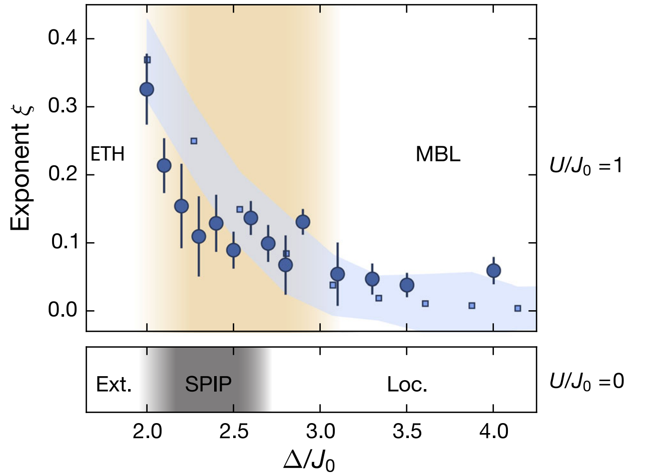

FIG. 3. Power-law exponents: Measured relaxation exponents as a function of the detuning strength for the GAA model at $U/J_0 = 1$. The error bars denote the uncertainty of the fit. The blue shaded region shows the result of numerical simulations including fit uncertainties, while the brown shaded area indicates a regime of slow dynamics with finite relaxation exponents reminiscent of the slow dynamics observed in the interacting AA model [50]. The lower part of the figure represents the situation in the noninteracting system which exhibits an extended and a localized phase as well as a single-particle intermediate phase whose numerically predicted width [51] is represented by the gray shaded region.

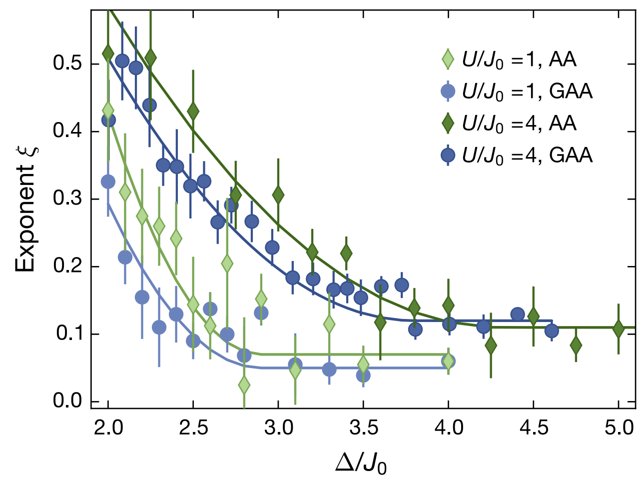

FIG. 4. Power-law exponents: Direct comparison of the relaxation exponents for both models and interaction strengths. Error bars denote the uncertainty of the fit. Solid lines are guides to the eye. The width of the corresponding SPIP for various lattice depths can be found in Ref. [51].

described by such power laws. For a detailed discussion of the applicability of this picture, see Ref. [50]. In the GAA model, we observe that the exponents reach a value of 0.33(5) just above the single-particle localization transition point; for larger detuning lattice strengths, the exponents decrease and finally converge to a constant positive plateau around $\Delta/J_0 = 3.0(2)$, which is significantly larger than the single-particle localization transition point $\Delta/J_0 \simeq 2.6$ [51]. Although the relaxation exponent is expected to be strictly zero ($\xi = 0$) in the MBL phase, we regard our system to be many-body localized in this regime and attribute the residual decay to the existence of external baths. Off-resonant photon scattering [56,60] and couplings between different 1D tubes [55] give rise to a finite imbalance lifetime even in the many-body localized phase. Moreover, the experimental exponents are in reasonably good agreement with numerical simulations in a system with $L = 16$ sites [51]. This observation implies that MBL indeed can occur in a system with an SPIP at least in a regime where the corresponding noninteracting model is fully localized (Fig. 3). A larger critical disorder strength is expected, since interactions tend to delocalize the system [25].

As pointed out above, below the single-particle localization transition, the imbalance decay is very fast, corresponding to a thermal phase. For intermediate detuning strengths between ETH and MBL, we observe slow dynamics (brown shaded area in Fig. 3), which are characterized by finite relaxation exponents. A similar intermediate phase of slow dynamics has been found previously in the interacting AA model [50]. In this intermediate phase of the GAA model, one could expect that the presence of extended states gives rise to a faster relaxation of the imbalance, since the single-particle extended states may act as a bath for the coexistent localized states, when coupled by interactions. In order to investigate this assumption, we compare the relaxation exponents of the GAA model and the AA model (Fig. 4), where a similar mechanism is expected to be absent. The dynamics turn out to be indistinguishable within the experimental uncertainties across all investigated detuning strengths. This fact provides an indication that the extended states in the noninteracting spectrum do not act as an effective bath thermalizing the whole system, at least within the timescales of our experiment. We also numerically investigate longer evolution times, where we find hints towards a faster relaxation in the intermediate regime in the GAA model, although this observation is not fully conclusive due to finite-size limitations [51].

It has been proposed that an MBIP may also exist at large interactions due to symmetry-constrained dynamics [11]. We perform measurements at stronger interactions $U/J_0 = 4$ again for both models as shown in Fig. 4 and Ref. [51]. The exponents at the same detuning strengths are overall larger at stronger interactions, accompanied by a shift of the critical disorder strength for MBL. Also, for the case of strong interactions we find that the exponents are remarkably similar.

Outlook.—We have experimentally and numerically investigated the localization transition of the GAA model in the presence of interactions. We find that, for large enough detuning lattice strengths, the system likely reaches the many-body localized phase when all single-particle states in the corresponding noninteracting limit have been localized. Furthermore, we compare the experimental relaxation exponents in the AA model and the GAA model for multiple detuning and interaction strengths and find that they are similar on short timescales in agreement with numerical simulations, indicating that the coexistent extended states do not serve as an efficient bath within the experimentally accessible timescales for the initial states probed in this work. Generally, our results do not rule out the existence of an MBIP, since the experiment is limited to finite times due to the presence of external baths, and the imbalance measurement alone may not be a reliable diagnostic to decisively detect it. Note, however, that these considerations are based on the assumption that no intermediate phase exists in the interacting AA model; however, the intermediate regime of slow dynamics [50] is not yet fully understood [61] and requires further investigations. A possible explanation of the qualitatively similar relaxation dynamics observed in this work could be that the mechanism responsible for the slow dynamics in both models is indeed of a similar physical origin. In the future, it is worthwhile to extend the experimental measurements to much longer times in order to investigate the stability of MBL and reveal potential delocalization mechanisms introduced by the spin degree of freedom [62–67]. In addition, it is desirable to find a definitive experimental diagnostic for the possible many-body intermediate phase, which is currently lacking.

We thank Ehud Altman for insightful discussions. We acknowledge financial support by the European Commission (UQUAM Grant No. 319278, AQuS), the Nanosystems Initiative Munich (NIM Grant No. EXC4), and the Deutsche Forschungsgemeinschaft (DFG, German Research Foundation) under Germany's Excellence Strategy—EXC-2111–39081486. X. L. also acknowledges support from City University of Hong Kong (Project No. 9610428). Furthermore, this work is supported at the University of Maryland by Laboratory for Physical Sciences and Microsoft.

[*]T. K., S. S., and X. L. contributed equally to this work.
[†]monika.aidelsburger@physik.uni-muenchen.de

[1] I. V. Gornyi, A. D. Mirlin, and D. G. Polyakov, Interacting Electrons in Disordered Wires: Anderson Localization and Low-T Transport, Phys. Rev. Lett. **95**, 206603 (2005).
[2] D. M. Basko, I. L. Aleiner, and B. L. Altshuler, Metal-insulator transition in a weakly interacting many-electron system with localized single-particle states, Ann. Phys. (Amsterdam) **321**, 1126 (2006).
[3] V. Oganesyan and D. A. Huse, Localization of interacting fermions at high temperature, Phys. Rev. B **75**, 155111 (2007).
[4] M. Žnidarič, T. Prosen, and P. Prelovšek, Many-body localization in the Heisenberg XXZ magnet in a random field, Phys. Rev. B **77**, 064426 (2008).
[5] A. Pal and D. A. Huse, Many-body localization phase transition, Phys. Rev. B **82**, 174411 (2010).
[6] J. H. Bardarson, F. Pollmann, and J. E. Moore, Unbounded Growth of Entanglement in Models of Many-Body Localization, Phys. Rev. Lett. **109**, 017202 (2012).
[7] S. Iyer, V. Oganesyan, G. Refael, and D. A. Huse, Many-body localization in a quasiperiodic system, Phys. Rev. B **87**, 134202 (2013).
[8] R. Nandkishore and D. A. Huse, Many-body localization and thermalization in quantum statistical mechanics, Annu. Rev. Condens. Matter Phys. **6**, 15 (2015).
[9] J. A. Kjäll, J. H. Bardarson, and F. Pollmann, Many-Body Localization in a Disordered Quantum Ising Chain, Phys. Rev. Lett. **113**, 107204 (2014).
[10] D. J. Luitz, N. Laflorencie, and F. Alet, Many-body localization edge in the random-field Heisenberg chain, Phys. Rev. B **91**, 081103(R) (2015).
[11] I. Mondragon-Shem, A. Pal, T. L. Hughes, and C. R. Laumann, Many-body mobility edge due to symmetry-constrained dynamics and strong interactions, Phys. Rev. B **92**, 064203 (2015).
[12] M. Serbyn, Z. Papić, and D. A. Abanin, Criterion for Many-Body Localization-Delocalization Phase Transition, Phys. Rev. X **5**, 041047 (2015).
[13] R. Modak and S. Mukerjee, Many-Body Localization in the Presence of a Single-Particle Mobility Edge, Phys. Rev. Lett. **115**, 230401 (2015).
[14] R. Nandkishore, Many-body localization proximity effect, Phys. Rev. B **92**, 245141 (2015).
[15] X. Li, S. Ganeshan, J. H. Pixley, and S. Das Sarma, Many-Body Localization and Quantum Nonergodicity in a Model with a Single-Particle Mobility Edge, Phys. Rev. Lett. **115**, 186601 (2015).
[16] X. Li, J. H. Pixley, D.-L. Deng, S. Ganeshan, and S. Das Sarma, Quantum nonergodicity and fermion localization in a system with a single-particle mobility edge, Phys. Rev. B **93**, 184204 (2016).
[17] K. Hyatt, J. R. Garrison, A. C. Potter, and B. Bauer, Many-body localization in the presence of a small bath, Phys. Rev. B **95**, 035132 (2017).
[18] D. J. Luitz, N. Laflorencie, and F. Alet, Extended slow dynamical regime close to the many-body localization transition, Phys. Rev. B **93**, 060201(R) (2016).
[19] J. Z. Imbrie, On many-body localization for quantum spin chains, J. Stat. Phys. **163**, 998 (2016).
[20] J. M. Deutsch, Quantum statistical mechanics in a closed system, Phys. Rev. A **43**, 2046 (1991).
[21] M. Srednicki, Chaos and quantum thermalization, Phys. Rev. E **50**, 888 (1994).
[22] J. Smith, A. Lee, P. Richerme, B. Neyenhuis, P. W. Hess, P. Hauke, M. Heyl, D. A. Huse, and C. Monroe, Many-body localization in a quantum simulator with programmable random disorder, Nat. Phys. **12**, 907 (2016).
[23] K. X. Wei, C. Ramanathan, and P. Cappellaro, Exploring Localization in Nuclear Spin Chains, Phys. Rev. Lett. **120**, 070501 (2018).

[24] K. Xu, J.-J. Chen, Y. Zeng, Y.-R. Zhang, C. Song, W. Liu, Q. Guo, P. Zhang, D. Xu, H. Deng, K. Huang, H. Wang, X. Zhu, D. Zheng, and H. Fan, Emulating Many-Body Localization with a Superconducting Quantum Processor, Phys. Rev. Lett. **120**, 050507 (2018).

[25] M. Schreiber, S. S. Hodgman, P. Bordia, H. P. Lüschen, M. H. Fischer, R. Vosk, E. Altman, U. Schneider, and I. Bloch, Observation of many-body localization of interacting fermions in a quasirandom optical lattice, Science **349**, 842 (2015).

[26] P. Roushan *et al.*, Spectroscopic signatures of localization with interacting photons in superconducting qubits, Science **358**, 1175 (2017).

[27] S. Aubry and G. André, Analyticity breaking and Anderson localization in incommensurate lattices, Ann. Isr. Phys. Soc. **3**, 133 (1980).

[28] G. Roati, C. D'Errico, L. Fallani, M. Fattori, C. Fort, M. Zaccanti, G. Modugno, M. Modugno, and M. Inguscio, Anderson localization in an non-interacting Bose-Einstein condensate, Nature (London) **453**, 895 (2008).

[29] S. Das Sarma, A. Kobayashi, and R. E. Prange, Proposed Experimental Realization of Anderson Localization in Random and Incommensurate Artificially Layered Systems, Phys. Rev. Lett. **56**, 1280 (1986).

[30] S. Ganeshan, J. H. Pixley, and S. Das Sarma, Nearest Neighbor Tight Binding Models with an Exact Mobility Edge in One Dimension, Phys. Rev. Lett. **114**, 146601 (2015).

[31] J. Biddle and S. Das Sarma, Predicted Mobility Edges in One-Dimensional Incommensurate Optical Lattices: An Exactly Solvable Model of Anderson Localization, Phys. Rev. Lett. **104**, 070601 (2010).

[32] J. Biddle, D. J. Priour, B. Wang, and S. Das Sarma, Localization in one-dimensional lattices with non-nearest-neighbor hopping: Generalized Anderson and Aubry-André models, Phys. Rev. B **83**, 075105 (2011).

[33] S. Das Sarma, S. He, and X. C. Xie, Mobility Edge in a Model One-Dimensional Potential, Phys. Rev. Lett. **61**, 2144 (1988).

[34] M. Griniasty and S. Fishman, Localization by Pseudorandom Potentials in One Dimension, Phys. Rev. Lett. **60**, 1334 (1988).

[35] S. Das Sarma, S. He, and X. C. Xie, Localization, mobility edges, and metal-insulator transition in a class of one-dimensional slowly varying deterministic potentials, Phys. Rev. B **41**, 5544 (1990).

[36] D. J. Thouless, Localization by a Potential with Slowly Varying Period, Phys. Rev. Lett. **61**, 2141 (1988).

[37] C. M. Soukoulis and E. N. Economou, Localization in One-Dimensional Lattices in the Presence of Incommensurate Potentials, Phys. Rev. Lett. **48**, 1043 (1982).

[38] X. Li, X. Li, and S. Das Sarma, Mobility edges in one-dimensional bichromatic incommensurate potentials, Phys. Rev. B **96**, 085119 (2017).

[39] H. P. Lüschen, S. Scherg, T. Kohlert, M. Schreiber, P. Bordia, X. Li, S. Das Sarma, and I. Bloch, Single-Particle Mobility Edge in a One-Dimensional Quasi-periodic Optical Lattice, Phys. Rev. Lett. **120**, 160404 (2018).

[40] F. A. An, E. J. Meier, and B. Gadway, Engineering a Flux-Dependent Mobility Edge in Disordered Zigzag Chains, Phys. Rev. X **8**, 031045 (2018).

[41] R. Modak, S. Ghosh, and S. Mukerjee, Criterion for the occurrence of many-body localization in the presence of a single-particle mobility edge, Phys. Rev. B **97**, 104204 (2018).

[42] Y.-T. Hsu, X. Li, D.-L. Deng, and S. Das Sarma, Machine Learning Many-Body Localization: Search for the Elusive Nonergodic Metal, Phys. Rev. Lett. **121**, 245701 (2018).

[43] M. Schecter, T. Iadecola, and S. Das Sarma, Configuration-controlled many-body localization and the mobility emulsion, Phys. Rev. B **98**, 174201 (2018).

[44] W. De Roeck, F. Huveneers, M. Müller, and M. Schiulaz, Absence of many-body mobility edges, Phys. Rev. B **93**, 014203 (2016).

[45] W. De Roeck and F. Huveneers, Stability and instability towards delocalization in many-body localization systems, Phys. Rev. B **95**, 155129 (2017).

[46] E. Baygan, S. P. Lim, and D. N. Sheng, Many-body localization and mobility edge in a disordered spin-$\frac{1}{2}$ Heisenberg ladder, Phys. Rev. B **92**, 195153 (2015).

[47] D. J. Luitz, Long tail distributions near the many-body localization transition, Phys. Rev. B **93**, 134201 (2016).

[48] E. J. Torres-Herrera and L. F. Santos, Extended nonergodic states in disordered many-body quantum systems, Ann. Phys. (Berlin) **529**, 1600284 (2017).

[49] S. Nag and A. Garg, Many-body mobility edges in a one-dimensional system of interacting fermions, Phys. Rev. B **96**, 060203(R) (2017).

[50] H. P. Lüschen, P. Bordia, S. Scherg, F. Alet, E. Altman, U. Schneider, and I. Bloch, Observation of Slow Dynamics Near the Many-Body Localization Transition in One-Dimensional Quasiperiodic Systems, Phys. Rev. Lett. **119**, 260401 (2017).

[51] See Supplemental Material at http://link.aps.org/supplemental/10.1103/PhysRevLett.122.170403 for details on experimental techniques, model parameters, additional data for strong interactions ($U/J_0 = 4$), additional data for a primary lattice depth $V_p = 3E_r^p$, a numerical phase diagram of the noninteracting GAA and AA models, a description of the numerical methods, and numerical data at longer evolution times, which includes Ref. [52].

[52] A. Weiße, G. Wellein, A. Alvermann, and H. Fehske, The kernel polynomial method, Rev. Mod. Phys. **78**, 275 (2006).

[53] J. Sebby-Strabley, M. Anderlini, P. S. Jessen, and J. V. Porto, Lattice of double wells for manipulating pairs of cold atoms, Phys. Rev. A **73**, 033605 (2006).

[54] S. Fölling, S. Trotzky, P. Cheinet, M. Feld, R. Saers, A. Widera, T. Müller, and I. Bloch, Direct observation of second-order atom tunnelling, Nature (London) **448**, 1029 (2007).

[55] P. Bordia, H. P. Lüschen, S. S. Hodgman, M. Schreiber, I. Bloch, and U. Schneider, Coupling Identical One-Dimensional Many-Body Localized Systems, Phys. Rev. Lett. **116**, 140401 (2016).

[56] H. P. Lüschen, P. Bordia, S. S. Hodgman, M. Schreiber, S. Sarkar, A. J. Daley, M. H. Fischer, E. Altman, I. Bloch, and U. Schneider, Signatures of Many-Body Localization in a

Controlled Open Quantum System, Phys. Rev. X **7**, 011034 (2017).

[57] R. B. Griffiths, Nonanalytic Behavior Above the Critical Point in a Random Ising Ferromagnet, Phys. Rev. Lett. **23**, 17 (1969).

[58] R. Vosk, D. A. Huse, and E. Altman, Theory of the Many-Body Localization Transition in One-Dimensional Systems, Phys. Rev. X **5**, 031032 (2015).

[59] S. A. Weidinger, S. Gopalakrishnan, and M. Knap, A self-consistent Hartree-Fock approach to many-body localization, Phys. Rev. B **98**, 224205 (2018).

[60] H. Pichler, A. J. Daley, and P. Zoller, Nonequilibrium dynamics of bosonic atoms in optical lattices: Decoherence of many-body states due to spontaneous emission, Phys. Rev. A **82**, 063605 (2010).

[61] S. Xu, X. Li, Y.-T. Hsu, B. Swingle, and S. Das Sarma, Butterfly effect in interacting aubry-andre model: Thermalization, slow scrambling, and many-body localization, arXiv:1902.07199.

[62] R. Vasseur, A. C. Potter, and S. A. Parameswaran, Quantum Criticality of Hot Random Spin Chains, Phys. Rev. Lett. **114**, 217201 (2015).

[63] A. C. Potter and R. Vasseur, Symmetry constraints on many-body localization, Phys. Rev. B **94**, 224206 (2016).

[64] P. Prelovšek, O. S. Barišič, and M. Žnidarič, Absence of full many-body localization in the disordered Hubbard chain, Phys. Rev. B **94**, 241104(R) (2016).

[65] I. V. Protopopov, W. W. Ho, and D. A. Abanin, Effect of SU(2) symmetry on many-body localization and thermalization, Phys. Rev. B **96**, 041122(R) (2017).

[66] M. Kozarzewski, P. Prelovšek, and M. Mierzejewski, Spin Subdiffusion in the Disordered Hubbard Chain, Phys. Rev. Lett. **120**, 246602 (2018).

[67] I. V. Protopopov and D. A. Abanin, Spin-mediated particle transport in the disordered hubbard model, Phys. Rev. B **99**, 115111 (2019).